

**Current Biology, Volume 22**

## **Supplemental Information**

### **Attention Modulates**

### **Spinal Cord Responses to Pain**

**Christian Sprenger, Falk Eippert, Jürgen Finsterbusch, Ulrike Bingel, Michael Rose,  
and Christian Büchel**

### **Supplemental Inventory**

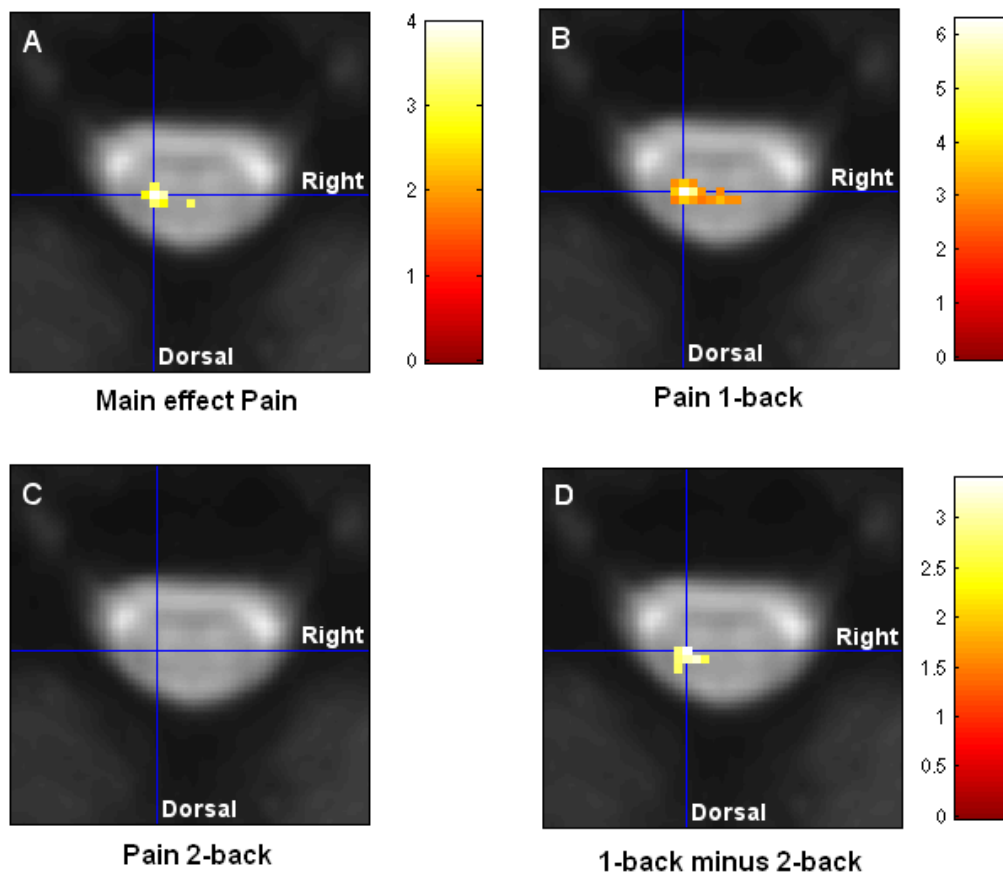
#### **1. Supplemental Figures**

Figure S1, related to Figure 2

Figure S2, related to Figure 3

#### **2. Supplemental Experimental Procedures**

#### **3. Supplemental References**



**Figure S1. Pain-Related BOLD Responses in the Cervical Spinal Cord, Related to Figure 2**

BOLD responses to painful stimulation at the spinal segment C6. Activation maps are overlaid on the mean functional (EPI) image of all subjects participating in experiment 1. The blue crosshairs label the peak voxel of the main effect of pain.

(A) Main effect of pain: the peak voxel is found in the dorsal horn, ipsilateral to the side of painful stimulation (left).

(B) 1-back: under low working memory load, we observed activation in the left dorsal horn.

(C) 2-back: no such activation could be detected under high working memory load.

(D) Differential contrast (1-back minus 2-back): we observed a distinct cluster in the ipsilateral dorsal horn. The color bars indicate t values, and the visualization threshold is set to  $p < 0.01$ .

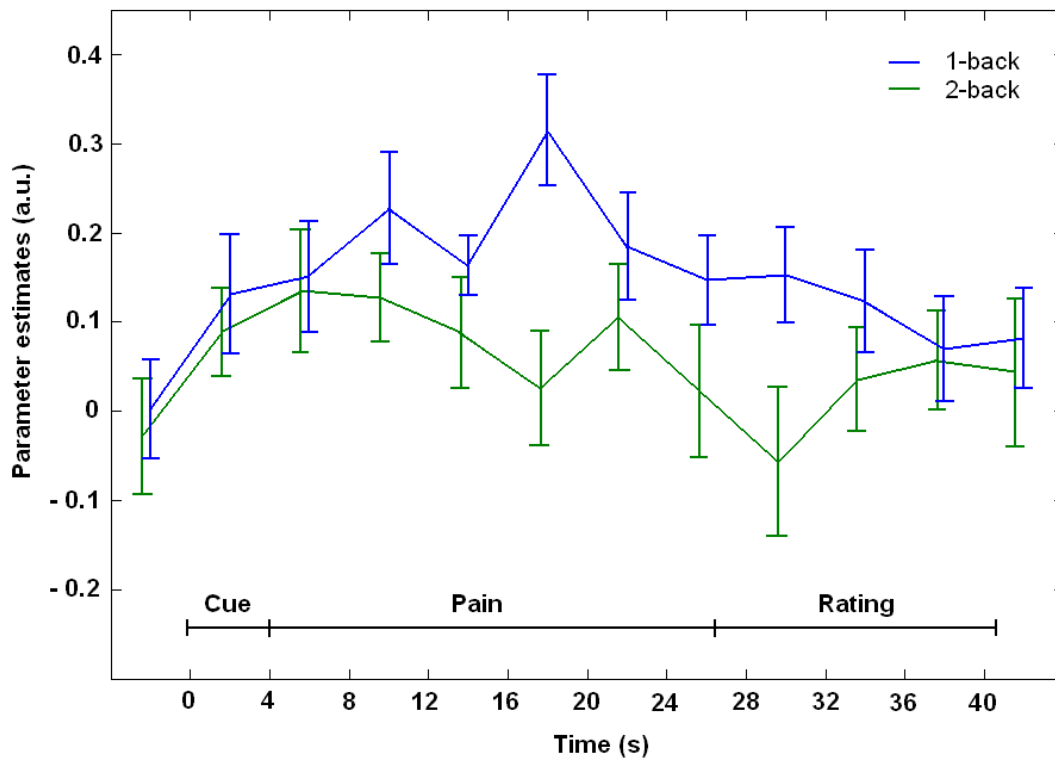


**Figure S2. Peri-Stimulus Time Course, Related to Figure 3**

The panel shows the time course of the response at the peak voxel of the main effect of pain (averaged over all blocks, separately for each condition). The time course of the high working memory load condition was shifted slightly to the left to avoid overlapping of error bars. Both time courses were obtained from an analysis that used FIRs as basis functions and does not make any a priori assumptions about the shape of the hemodynamic response. Error bars indicate standard errors.

## **Supplemental Experimental Procedures:**

### **Subjects**

Given reports that pain perception and possibly the effect of the opioidergic system is affected by the menstrual cycle, we only included male volunteers. Exclusion criteria were any history of neurological disease, including any history of pain syndrome and any form of spinal cord ailment. In experiment 1 data from 3 of the 20 subjects had to be discarded because of incorrect MRI scanning adjustment (one subject), failure of the automatic spatial normalization procedure (one subject) and artifacts in physiological data (one subject). Subjects were characterized by following questionnaires: Beck Depression Inventory [1] (experiment 1:  $2.12 \pm 0.34$ ; experiment 2:  $3.33 \pm 0.36$ ), Crowne-Marlowe Social Desirability Scale [2] (experiment 1:  $11.2 \pm 0.86$ ; experiment 2:  $12.9 \pm 0.96$ ), Pain catastrophizing scale [3] (experiment 1:  $20.87 \pm 2.10$ ; experiment 2:  $24.86 \pm 2.08$ ) and the State-Trait Anxiety Inventory [4] (experiment 1:  $33.1 \pm 1.3$ ; experiment 2:  $35.5 \pm 0.95$ ).

### **Experimental Paradigm**

The experimental paradigm combined two levels of a well-established n-back working memory task with painful heat stimulation of fixed physical intensity to the left forearm. Subjects were told that the study investigated central neuronal processing in the context of working memory and concentrativeness. Subjects were also told that they would receive a task-irrelevant pain stimulus to the left forearm. Importantly, it was not mentioned to the subjects that the working memory task could exert an effect on perceived pain intensity, as this might have led to a confounding effect of social desirability.

Prior to the each experiment, for each subject we determined the individual temperature that would elicit the intended pain level of  $\sim 60$  on a visual analogue scale (VAS; 0-100, endpoints “no pain” - “unbearable pain”). Therefore we applied several 22.5s long painful stimuli to their right forearm. As a starting point, we used a temperature of  $47.5\text{ }^{\circ}\text{C}$  and then increased or decreased the temperature for the next stimulus in steps of 0.5 degrees until a pain level of approximately 60 was reached. The group average of temperature for the pain level of 60 on the VAS was  $47.3\text{ }^{\circ}\text{C} \pm 0.1$  (mean $\pm$ SEM) in experiment 1. In experiment 2 we determined the individual temperature that would elicit the pain level of  $\sim 60$  on a VAS in the same manner on day one and applied this temperature on both study days. The group average of temperature for the pain level of 60 in experiment 2 was  $47.0\text{ }^{\circ}\text{C} \pm 0.1$  (mean $\pm$ SEM).

Subjects were also familiarized with the n-back task (see below) and practised it until a satisfactory level of performance (at least 2 of 5 n-back test-blocks correct) was reached. The experiment itself consisted of 1 session ( $\sim 25$  min.) comprising 24 blocks. Half of the blocks comprised a 1-back task inducing a low level of working memory load and the other half comprised a 2-back task inducing high working memory load. The presentation order of the blocks was randomized. Each single block consisted of an anticipation period (4s), a pain stimulation accompanied by the n-back task (22.5s), a rating period (14s) and finally a variable inter-trial interval (15-25s) (see Figure 1 in the main text). During the anticipation phase, a visual cue (“One-Back” respectively “Two-Back”) indicated whether a 1-back or 2-back task should be performed in the following period. During the next part the painful heat stimulus ( $\sim 1.5$ s ramp up, 19.5s plateau,  $\sim 1.5$ s ramp down, using the previously determined temperature) was administered to the left radial forearm below the crook of the arm (receptive field of the n. cutaneus antibrachii lateralis, dermatome C6). Subjects were not told that the physical intensity of the stimuli actually remained identical throughout the experiment and no hints regarding potential differences in perceived pain intensity were given. Simultaneously to the noxious stimulation subjects had to perform the 1-back or the 2-

back working memory task. Here a 1-back target is defined as a match between the actual letter and the directly preceding letter, whereas a 2-back target is defined as a match between the actual letter and the letter preceding this one by two letters. The letters that comprised the stimulus material of this task were always presented centrally on the screen, which subjects could see via a tilted mirror mounted on the head coil. Only the letters A, B, C, D, E were used. A total number of 15 letters appeared during the 22.5s period (each letter was visible for 750ms, followed by a pause of 750ms). To minimize the influence of movement on the fMRI measurement during pain stimulation in experiment 1 subjects indicated the hits not by button press immediately after detection, but rated the sum of n-back hits directly after the pain stimulation by selecting the supposed number of hits from a choice (from 0 to 5 hits); the same procedure was used in experiment 2. Note that this additional amount of working memory load was identical for both conditions as the mean number of targets was equal for both conditions. Pilot data had shown that this modified n-back task (shorter display time and the need of summing up all hits, which both enhances difficulty) leads to an effective behavioral hypoalgesia under the high working memory load condition. Subsequently, subjects had to rate the pain intensity present during that block, using a VAS (see above). Subjects had to execute all button presses with their right index finger. A variable intertrial interval ( $20 \pm 5$ s) followed, during which a white cross-hair was displayed. Finally subjects were paid for their participation.

### **Drug Administration and Adverse Effects of Naloxone (Experiment 2)**

Fifteen minutes before the behavioral paradigm started, a bolus of 0.15 mg naloxone (Naloxon-ratiopharm, Ratiopharm GmbH, Ulm, Germany) per kg bodyweight or the same amount of 0.9% saline solution was intravenously administered. This dose has shown reliable naloxone effects in several previous studies [5, 6] and is sufficient to block central opioid receptors completely [7]. Because of the relatively short half-life period of naloxone, an additional constant intravenous infusion (dose of 0.2 mg/kg/h or saline for the duration of the experiment) was administered, starting shortly after bolus administration. This regimen leads to stable naloxone plasma concentrations [8].

Subjects answered a 7-item questionnaire regarding potential adverse effects of naloxone at the end of each study day. This questionnaire has been employed in previous neuropharmacological studies [9–12]. Each adverse effect could be rated as “inexistent”, “very weak”, “weak”, “moderate”, “strong”, “very strong”, and “extremely strong” (scores: 0-6). To test for differences between both study days, we used Wilcoxon rank sum tests. Group scores were generally very low and no significant differences between the saline and naloxone application were observed.

After answering the adverse effects questionnaire subjects had to rate their present mood on a 17-item questionnaire which has also been employed in previous neuropharmacological studies [9–12]. Each item consisted of a visual analogue scale (0-100) with opposing verbal termini at each end. To test for differences between both study days, we used a paired t-test. Again no significant differences between the saline and naloxone application were found.

### **MRI Data Acquisition**

MRI data acquisition was similar to a previous fMRI study on pain processing of the human spinal cord [13]. Subjects were positioned in a 12-channel head coil combined with a 4-channel neck coil (both receive-only) with the target region of the spinal cord being centred

in the magnet's isocenter. To minimize head and neck movements we used a vendorsupplied vacuum immobilization mat to stabilize the position of the cervical vertebrae.

High-resolution ( $1 \times 1 \times 1 \text{mm}^3$ ) T1-weighted anatomical images were acquired using a 3D-MPRAGE sequence (sagittal slice orientation, repetition time 2.3s, echo time 3.43ms, readout flip angle  $9^\circ$ , inversion time 1.1s, field-of-view  $192 \times 240 \times 256 \text{mm}^3$ ). The field of view ranged from the midbrain to the second thoracic vertebra. For this acquisition, both coils were used, whereas for the acquisition of functional images we only used the neck coil. Functional images were acquired using a gradient-echo echo-planar imaging (EPI) sequence (repetition time: 1170 ms, echo time: 42ms, flip angle:  $70^\circ$ , field of view:  $128 \times 128 \text{mm}^2$ , matrix:  $128 \times 128$ ; GRAPPA with a PAT-factor of 2 and 24 reference lines). The target volume covered an area from the middle part of the fourth cervical vertebra to the lower part of the sixth cervical vertebra, including the spinal segments C5, C6 and the upper part of C7. We acquired 10 slices positioned approximately perpendicular to the spinal cord, using a slice thickness of 5mm in order to achieve an adequate signal-to-noise ratio despite a high in-plane resolution ( $1 \times 1 \text{mm}^2$ ).

To minimize sensitivity to flow effects, flow rephasing in slice direction and spatially-selective saturation pulses superior and inferior to the target volume were used and the images obtained with the individual coil channels were combined with a sum-of-squares algorithm. Furthermore, additional saturation pulses were applied posterior and anterior to the target region, i.e. in the phase-encoding direction, in order to avoid ghosting and minimize inflow artifacts related to pulsatile blood flow in major vessels.

To minimize signal intensity variations caused by magnetic susceptibility differences (e.g. between the intervertebral discs and vertebral bodies) for each subject a slice-specific z-shim gradient momentum was used. It was determined based on a pre-scan with 21 different gradient moments applied to all slices by selecting the gradient setting yielding the maximum intensity within the chosen spinal cord region-of-interest [14].

The first 10 volumes were discarded in order to eliminate T1 saturation effects. To allow for retrospective physiological noise correction [15], which is critical in spinal fMRI [16, 17], heart-rate and respiration-rate data were measured using the vendorsupplied pulse sensor and respiratory belt and were recorded on the scanner together with the trigger pulses to ensure timing accuracy.

### **Behavioral Data Analysis**

All behavioral data were analyzed in MATLAB 7.7 (MathWorks, USA). The analgesic effect by working memory load was calculated as the difference between the mean pain ratings during the 1-back condition and the 2-back condition (1-back minus 2-back). As we had the strong a priori hypothesis that distraction would reduce pain perception, we used a one-tailed paired t-test to statistically test for reduced pain ratings during the 2-back condition compared to the 1-back condition. To test for a difference in the analgesic effect between the naloxone treatment and the saline application, we used a two-tailed paired t-test. The estimated task performance was calculated as the ratio of correct blocks to the total amount of blocks for each working memory condition separately (12 blocks each). To test for a difference in the estimated task performance between the 2-back condition compared to the 1-back condition as well as for a difference in the estimated task performance between saline and naloxone application, we used a paired t-test (two-tailed). Robust regression was calculated to examine the relationship between BOLD-changes in the dorsal horn and behavioral pain reductions. For all behavioral analyses results were considered significant at  $p < 0.05$ .

## **fMRI Data Analysis**

fMRI data preprocessing and statistical analyses were carried out using statistical parametric mapping (SPM8, Wellcome Trust Centre for Neuroimaging, London, UK). Motion correction was performed using a standard rigid body transformation as employed in SPM (six degrees of freedom). To minimize the influence of neck and shoulder muscles on the motion correction procedure [18], the cost function was weighted by an automatically created mask (using morphological procedures implemented in Matlab's Image Processing Toolbox) that only included the spinal cord and surrounding tissue. Within this mask, highly variant regions (i.e. CSF) were excluded, to base the registration procedure only on spinal cord movement. In order to perform group analyses, we also spatially normalized the data. Therefore we used a single subject template of the human spinal cord from a previous fMRI study [13]. We used the standard SPM normalization algorithm (including both affine and non-linear terms) to normalize the T1-weighted images from all other subjects onto this subject's T1-weighted image. The obtained parameters were then applied to the functional images, which were resampled at a resolution of  $1 \times 1 \times 1 \text{mm}^3$ . The structural images were then averaged and the resulting mean image was used for localization of BOLD responses. Additionally, we created a mean group functional (EPI) image from the individual normalized functional images, which was also used for displaying results in a transversal plane. Finally, the functional images were smoothed with a 2 mm (FWHM) isotropic Gaussian kernel, which was used as a compromise to facilitate group analysis, but at the same time to allow an appropriate anatomical assignment. Data were also subjected to temporal high-pass filtering (cutoff period: 128s).

Data analysis was performed using a general linear model (GLM) approach. The first-level design matrix of each subject included the following regressors: anticipation 1-back, anticipation 2-back, pain 1-back, pain 2-back, rating 1-back, rating 2-back, estimated movement parameters (3 translations and 3 rotations), 21 physiological noise regressors (see below) and one constant. The regressors representing the experimental paradigm were modelled by convolving boxcar functions for each regressor (anticipation duration: 4s, pain duration: 22.5s, rating duration: 14s) with the canonical hemodynamic response function (HRF).

We then defined adequate first-level contrasts to test for a) the main effect of pain, b) pain 1-back, c) pain 2-back, d) pain 1-back > pain 2-back. After model estimation, the ensuing contrast images from each subject were used for second-level analyses using one-sample t-tests. As we had no a priori hypotheses regarding the anticipation period and the rating phase we only investigated the different pain conditions in the second level analysis. In analogy to previous fMRI studies on pain processing [13, 19], data are reported at an uncorrected threshold of  $p < 0.005$ .

As the influence of physiological noise, which mainly arises from cardiac and respiratory sources, is much stronger in the spinal cord than in the brain [16, 17, 20, 21], we also corrected for this potential confound. We used the selective averaging method described by Deckers et al. [22] to generate regressors representing cardiac and respiratory effects (using 10 bins for cardiac and respiratory effects, respectively). Following the procedures outlined in Brooks et al. [17], we also aimed to correct for low-frequency noise by using the average CSF signal as a regressor; our procedure only differed from that of Brooks et al. [17] in that we included voxels whose variance lay in the top 25th percentile. Regressors representing cardiac, respiratory, and low frequency effects were thus also included in the first-level design matrix of each subject.

## Supplemental References:

1. Beck, A. T., Ward, C. H., and Mendelson, M. (1961). An inventory for measuring depression. *Archives of general psychiatry* 4, 561.
2. Crowne, D. P., and Marlowe, D. (1960). A new scale of social desirability independent of psychopathology. *Journal of consulting psychology* 24, 349.
3. Sullivan, M. J., Bishop, S. R., and Pivik, J. (1995). The pain catastrophizing scale: Development and validation. *Psychological assessment* 7, 524.
4. Spielberger, C. D. (1970). *State-Trait Anxiety Inventory*.
5. Amanzio, M., and Benedetti, F. (1999). Neuropharmacological dissection of placebo analgesia: expectation-activated opioid systems versus conditioning-activated specific subsystems. *The Journal of neuroscience* 19, 484.
6. Eippert, F., Bingel, U., Schoell, E., Yacubian, J., and Büchel, C. (2008). Blockade of endogenous opioid neurotransmission enhances acquisition of conditioned fear in humans. *The Journal of Neuroscience* 28, 5465.
7. Mayberg, H. S., and Frost, J. J. (1990). Opiate receptors. In *Quantitative imaging: neuroreceptors, neurotransmitters, and enzymes* (New York: Raven Press), pp. 81–95.
8. Schoell, E. D., Bingel, U., Eippert, F., Yacubian, J., Christiansen, K., Andresen, H., May, A., Buechel, C., and Greenlee, M. W. (2010). The effect of opioid receptor blockade on the neural processing of thermal stimuli. *PloS one* 5, e12344.
9. Bentley, P., Husain, M., and Dolan, R. J. (2004). Effects of cholinergic enhancement on visual stimulation, spatial attention, and spatial working memory. *Neuron* 41, 969–982.
10. Pessiglione, M., Seymour, B., Flandin, G., Dolan, R. J., and Frith, C. D. (2006). Dopamine-dependent prediction errors underpin reward-seeking behaviour in humans. *Nature* 442, 1042–1045.
11. Petrovic, P., Pleger, B., Seymour, B., Klöppel, S., De Martino, B., Critchley, H., and Dolan, R. J. (2008). Blocking central opiate function modulates hedonic impact and anterior cingulate response to rewards and losses. *The Journal of Neuroscience* 28, 10509.
12. Eippert, F., Bingel, U., Schoell, E. D., Yacubian, J., Klinger, R., Lorenz, J., and Buchel, C. (2009). Activation of the opioidergic descending pain control system underlies placebo analgesia. *Neuron* 63, 533–543.
13. Eippert, F., Finsterbusch, J., Bingel, U., and Büchel, C. (2009). Direct evidence for spinal cord involvement in placebo analgesia. *Science* 326, 404.
14. Finsterbusch, J., and Eippert, F. (2011). Slice-Specific Gradient Compensation of Magnetic Field Inhomogeneities to Improve T2\*-Weighted Imaging of the Human Spinal Cord. In *Proc. Intl. Soc. Magn. Reson. Med., 19th Annual Meeting* (Montreal, Canada), p. p. 3610.
15. Glover, G. H., Li, T. Q., and Ress, D. (2000). Image-based method for retrospective correction of physiological motion effects in fMRI: RETROICOR. *Magnetic Resonance in Medicine* 44, 162–167.
16. Piché, M., Cohen-Adad, J., Nejad, M. K., Perlberg, V., Xie, G., Beaudoin, G., Benali, H., and Rainville, P. (2009). Characterization of cardiac-related noise in fMRI of the cervical spinal cord. *Magnetic resonance imaging* 27, 300–310.



17. Brooks, J. C. ., Beckmann, C. F., Miller, K. L., Wise, R. G., Porro, C. A., Tracey, I., and Jenkinson, M. (2008). Physiological noise modelling for spinal functional magnetic resonance imaging studies. *Neuroimage* 39, 680–692.
18. Stroman, P. W., Nance, P. W., and Ryner, L. N. (1999). BOLD MRI of the human cervical spinal cord at 3 tesla. *Magnetic Resonance in Medicine* 42, 571–576.
19. Wager, T. D., Rilling, J. K., Smith, E. E., Sokolik, A., Casey, K. L., Davidson, R. J., Kosslyn, S. M., Rose, R. M., and Cohen, J. D. (2004). Placebo-induced changes in FMRI in the anticipation and experience of pain. *Science* 303, 1162.
20. Stroman, P. W. (2005). Magnetic resonance imaging of neuronal function in the spinal cord: spinal FMRI. *Clinical Medicine & Research* 3, 146.
21. Giove, F., Garreffa, G., Giulietti, G., Mangia, S., Colonnese, C., and Maraviglia, B. (2004). Issues about the fMRI of the human spinal cord. *Magnetic resonance imaging* 22, 1505–1516.
22. Deckers, R. H., van Gelderen, P., Ries, M., Barret, O., Duyn, J. H., Ikonomidou, V. N., Fukunaga, M., Glover, G. H., and de Zwart, J. A. (2006). An adaptive filter for suppression of cardiac and respiratory noise in MRI time series data. *Neuroimage* 33, 1072–1081.